JVI Journals.ASM.org

Self-Association of Lymphocytic Choriomeningitis Virus Nucleoprotein Is Mediated by Its N-Terminal Region and Is Not Required for Its Anti-Interferon Function

Emilio Ortiz-Riaño,[a] Benson Yee Hin Cheng,[a] Juan C. de la Torre,[b] and Luis Martínez-Sobrido[a]

Department of Microbiology and Immunology, University of Rochester, Rochester, New York, USA,[a] and Department of Immunology and Microbial Science, The Scripps Research Institute, La Jolla, California, USA[b]

Arenaviruses have a bisegmented, negative-strand RNA genome. Both the large (L) and small (S) genome segments use an ambisense coding strategy to direct the synthesis of two viral proteins. The L segment encodes the virus polymerase (L protein) and the matrix Z protein, whereas the S segment encodes the nucleoprotein (NP) and the glycoprotein precursor (GPC). NPs are the most abundant viral protein in infected cells and virions and encapsidate genomic RNA species to form an NP-RNA complex that, together with the virus L polymerase, forms the virus ribonucleoprotein (RNP) core capable of directing both replication and transcription of the viral genome. RNP formation predicts a self-association property of NPs. Here we document self-association (homotypic interaction) of the NP of the prototypic arenavirus lymphocytic choriomeningitis virus (LCMV), as well as those of the hemorrhagic fever (HF) arenaviruses Lassa virus (LASV) and Machupo virus (MACV). We also show heterotypic interaction between NPs from both closely (LCMV and LASV) and distantly (LCMV and MACV) genetically related arenaviruses. LCMV NP self-association was dependent on the presence of single-stranded RNA and mediated by an N-terminal region of the NP that did not overlap with the previously described C-terminal NP domain involved in either counteracting the host type I interferon response or interacting with LCMV Z.

Arenaviruses chronically infect rodents worldwide, and human infections can occur when individuals are exposed to aerosol forms of the virus or after direct contact between infectious materials and abraded skin. Several arenaviruses cause hemorrhagic fever (HF) disease in humans and pose a serious public health problem in their regions of endemicity (7, 27, 38). The Old World (OW) Lassa virus (LASV), the causative agent of Lassa fever (LF), is the HF arenavirus with the largest impact on public health, as it infects several hundred thousand people yearly in West Africa, resulting in high morbidity and significant mortality (8, 14). Moreover, increased traveling to and from regions of endemicity has resulted in importation of LF cases in metropolitan areas of regions where it is not endemic (18). On the other hand, increasing evidence indicates that the globally distributed OW arenavirus lymphocytic choriomeningitis virus (LCMV) is a neglected human pathogen of clinical significance (2, 12, 19, 30). In addition, several arenaviruses have been included as category A agents because of their potential use as agents of bioterrorism (3, 8). Public health concerns posed by human arenavirus infections are aggravated because of the lack of FDA-licensed arenavirus vaccines and because current therapeutic intervention is limited to an off-labeled use of the nucleoside analog ribavirin, which is only partially effective and associated with significant side effects (20, 28, 29, 41, 44). Therefore, it is important to develop novel antiviral strategies to combat human pathogenic arenaviruses, a task that would be facilitated by a detailed understanding of the arenavirus molecular and cell biology.

Arenaviruses are enveloped viruses with a bisegmented, negative-strand RNA genome. Both the large (L) and small (S) genome segments use an ambisense coding strategy to direct the synthesis of two viral proteins with opposite orientations (3, 7). The L segment encodes the RNA-dependent RNA polymerase (L protein) and the matrix-like protein (Z), the latter of which participates in the formation of the virion structure and is also the driving force of arenavirus budding (11, 33). The S segment encodes the glycoprotein precursor (GPC) and the nucleoprotein (NP). The GPC is posttranslationally processed to produce GP-1 and GP-2. These two subunits associate to form the glycoprotein complex (GP) that forms the spikes observed on the surface of the virion structure and mediate receptor recognition and cell entry (5, 7). The NP, the most abundant viral protein in both infected cells and virions, is the main component of the virus ribonucleoprotein (RNP), and the NP and the L protein constitute the minimal *trans*-acting viral factors required for viral RNA replication and gene transcription (22, 39).

Evidence indicates that the NP plays a variety of critical roles in arenavirus biology. Besides its critical role in viral RNA synthesis, the NP was found to exhibit an anti-interferon (anti-IFN) activity via an early blockade of IFN regulatory factor 3 (IRF3) (4, 25, 26). This anti-IFN activity was mapped at the C-terminal region of the NP (24), a region which contains a functional exonuclease-folding domain whose activity was linked to the anti-IFN activity of the NP (16, 40). The NP has also been suggested to interact with the Z protein to mediate the incorporation of viral RNPs into matured infectious virions (23, 37, 43). As with other negative-strand RNA viruses, the arenavirus NP's ability to interact with itself is predicted to be required for NP-mediated encapsidation of arenavi-

Received 23 June 2011 Accepted 28 December 2011
Published ahead of print 18 January 2012
Address correspondence to Luis Martínez-Sobrido, luis_martinez@urmc.rochester.edu, or Juan C. de la Torre, juanct@scripps.edu.

doi:10.1128/JVI.05503-11

rus genome RNA species, a critical step in the formation of functional RNPs. In this regard, a recent report documented that a 28-amino-acid region (residues 92 to 119) predicted to form a coiled-coil domain within the N-terminal region of the NP of the New World (NW) arenavirus Tacaribe virus (TCRV) mediates NP-NP interaction (23). Because homologous proteins from TCRV and LCMV have been shown to exhibit different functional properties (24), we examined whether the same NP region reported for TCRV was also involved in self-association of the LCMV NP. In this work, we provide experimental evidence that LCMV NP self-association is also directed by its N-terminal region, with the first 50 N-terminal residues and residues within the region covered by amino acids 308 to 358 playing a critical role in LCMV NP-NP interaction. These findings also indicate that the anti-IFN activity associated with many arenavirus (but not TCRV) NP proteins (24) and the ability of the NP to be incorporated into matured infectious virions (23, 37, 43) do not require NP-NP interaction. Moreover, we show that the LCMV NP is able to interact with NPs of both closely (LASV) and distantly (Machupo virus [MACV]) genetically related arenaviruses, suggesting the possibility of a conserved interacting domain within the N-terminal region of arenavirus NPs and the possibility of targeting NP-NP interaction to find antivirals for the treatment of arenavirus infections.

MATERIALS AND METHODS

Cells. Human embryonic kidney (293T) cells (ATCC CRL-11268) and Madin-Darby canine kidney (MDCK) cells (ATCC CCL-34) were maintained in Dulbecco's modified Eagle's medium (DMEM) supplemented with 10% fetal bovine serum, L-glutamine (2 mM), penicillin (100 units/ml), and streptomycin (100 μg/ml) in a 5% CO_2 atmosphere at 37°C.

Plasmids. (i) Generation of tagged NP proteins. The pCAGGs multicloning site (MCS) plasmid (35) was modified by cloning the hemagglutinin (HA) and FLAG epitope tags to allow N- or C-terminally tagged fusion constructs, as previously described (31). LCMV, LASV, and MACV NP open reading frames (ORFs) were amplified by PCR from pCAGGs plasmids containing C-terminally HA-tagged NPs (25) and cloned into the modified tagged pCAGGs plasmids using standard cloning techniques to obtain N- or C-terminally tagged forms of the indicated arenavirus NPs. All the N- and C-terminally tagged pCAGGs expression plasmids with HA or FLAG tags that were used in the coimmunoprecipitation (Co-IP) assays contain full-length, wild-type versions of LCMV, LASV, and MACV NPs.

(ii) Generation of plasmids for the mammalian two-hybrid (M2H) system. The herpes simplex virus VP16 transactivating domain and the GAL4 DNA-binding domain ORFs were amplified by PCR and cloned into the pCAGGs MCS vector (35) to generate pCAGGs VP16 and GAL4 plasmids containing two flanking MCS, allowing N- and C-terminal fusions to arenavirus NPs. Previously described N-terminal, C-terminal, and IFN-deficient LCMV NP mutants (24) were subcloned into the pCAGGs VP16 plasmid to generate C-terminal fusions to VP16. Residues on the LCMV NP corresponding to the recently described 3′ to 5′ exonuclease catalytic sites of the LASV NP (16, 40) were replaced by alanine (D382A, E384A, D459A, H517A, and D522A) by site-directed mutagenesis (Stratagene) and then subcloned into the pCAGGs VP16 plasmid. The pG5Luc reporter plasmid (Promega) was modified by fusing a green fluorescent protein (GFP) ORF to the N-terminal region of a firefly luciferase (FFL) coding sequence to generate pG5 GFP/Luc.

(iii) Generation of plasmids for bimolecular fluorescence complementation (BiFC) studies. N-terminal (EYN) and C-terminal (EYC) sequences of a yellow fluorescent protein (YFP) ORF were amplified by PCR from pCAGGs EYN-NS1 and pCAGGs EYC-NS1 plasmids (gifts from Juan Ayllón and Adolfo García-Sastre, Mount Sinai School of Medicine, NY) and cloned into the pCAGGs MCS vector (35) to generate pCAGGs EYN and pCAGGs EYC, respectively, which contain two flanking MCS for N- and C-terminal fusions. The LCMV NP was subcloned from previously described plasmids into EYN and EYC pCAGGs expression plasmids, generating N- and C-terminal fusion proteins.

Primers for the generation of the described constructions are available upon request. The coding regions of the generated constructs were verified by DNA sequencing.

Co-IP. 293T cells (3×10^6) were cotransfected in a suspension in 6-well tissue culture plates with 4 μg total of tagged NP pCAGGs expression plasmids per well by using Lipofectamine 2000 (Invitrogen) according to the manufacturer's instructions. An empty pCAGGs MCS plasmid was included to maintain a constant amount of transfected plasmid DNA. Forty-eight hours posttransfection, cells were collected by centrifugation at 14,000 rpm for 30 min at 4°C and lysed with 400 μl of lysis buffer (20 mM Tris-HCl [pH 7.4], 5 mM EDTA, 100 mM NaCl, 1% NP-40, and a complete cocktail of protease inhibitors; Roche) for 30 min on ice. Cell lysates were clarified by centrifugation at 14,000 rpm for 30 min at 4°C. Twenty microliters (5% of total cell lysates) was analyzed for protein expression by gel electrophoresis and Western blotting. For immunoprecipitation, 50 μl of EZview Red anti-HA or EZview Red anti-FLAG M2 affinity gel (Sigma) was preincubated for 10 min with lysis buffer at room temperature and used to immunoprecipitate 50 μl (12.5% of total cell lysates) of cleared lysates at 4°C overnight. Affinity gels were washed four times with 500 μl of lysis buffer, and immunoprecipitated samples were resuspended in 50 μl of sodium dodecyl sulfate-polyacrylamide gel electrophoresis (SDS-PAGE) loading buffer. A 25-μl aliquot of each immunoprecipitated sample was analyzed by Western blotting. For the *in vitro* reconstitution of LCMV NP-NP interaction, 50 μl of cell lysates from individually plasmid-transfected cells containing FLAG-tagged LCMV NP was mixed with 50 μl of cell lysates containing HA-tagged LCMV NP and incubated for 2 h at room temperature. Negative controls (single-plasmid-transfected cell lysates) and positive controls (extracts from double-plasmid-transfected cells) were included. For the RNase treatment experiment, 50 μl of cell lysates was incubated with RNases A (1 mg/ml) and T1 (80 U/ml) and/or RNase V1 (8 U/ml) for 2 h at room temperature before performing the coimmunoprecipitations. For LCMV NP oligomerization assays, cell extracts from 293T cells transfected with 2 μg of FLAG-tagged LCMV NP pCAGGs were analyzed by SDS-PAGE in the presence (+) or absence (−) of 2-mercaptoethanol (BME) at a final concentration of 1.5%.

Protein gel electrophoresis and Western blot analysis. Proteins were separated by 7.5% or 12% SDS-PAGE and then transferred onto nitrocellulose membranes (Bio-Rad) overnight at 4°C. After blocking for 1 h at room temperature with 10% dry milk in 1× phosphate-buffered saline (1× PBS), membranes were incubated with monoclonal and polyclonal primary antibodies (MAb and PAb, respectively) against HA and FLAG (Sigma; H9658, H6908, F1804-5, F7425), polyclonal antibody against VP16 (Sigma; V4388), monoclonal antibody against glyceraldehyde-3-phosphate dehydrogenase (GAPDH) (AbCAM; AB9484), and polyclonal antibody against GFP (Santa Cruz; SC8334) for 1 h at room temperature. Membranes were then washed three times with 1× PBS containing 0.1% Tween 20 and probed with secondary horseradish peroxidase-conjugated anti-mouse or anti-rabbit immunoglobulin (Ig) antibodies (GE Healthcare, United Kingdom) for 1 h at room temperature. After 3 washes with 1× PBS containing 0.1% Tween 20, proteins were detected using a chemiluminescence kit and autoradiography films from Denville Scientific, Inc. Protein band intensities were quantified using ImageJ software (National Institutes of Health [NIH]). Because intensities of HA and FLAG tag expression constructs varied based on the N- or C-terminal fusion, normalization of band quantifications was performed as follows.

(i) Input Western blots. For HA tag detection, a control intensity (100%) was assigned to either the N- or C-terminal HA fusion proteins when they were cotransfected in the presence of the pCAGGs MCS empty plasmid. Band intensities of the remaining lanes were normalized with

respect to the control intensity. Similarly, for the FLAG-tagged constructs, band intensities were normalized to the control intensity (N- or C-terminal FLAG fusion proteins cotransfected with the empty pCAGGs MCS plasmid). A GAPDH control intensity (100%) was assigned arbitrarily to one lane and used to normalize the remaining lanes.

(ii) Coimmunoprecipitation assays. The normalization of the immunoprecipitated HA- or FLAG-tagged NPs was performed similarly to the quantification of the input Western blots. Briefly, cell extracts immunoprecipitated with anti-HA (α-HA) (or α-FLAG) antibodies and probed with α-HA (or α-FLAG) antibodies were assigned a control intensity of 100%. The remaining lanes were normalized to their respective control intensity. For the normalization of the coimmunoprecipitated bands, a control intensity (100%) was assigned to immunoprecipitations with α-HA antibodies probed with α-FLAG. Similar quantifications were used for coimmunoprecipitations using α-FLAG that were probed with α-HA antibodies.

(iii) Oligomerization assay. A GAPDH control intensity (100%) was assigned arbitrarily to one lane and used to normalize the remaining lanes.

M2H system. 293T cells (6.5×10^5) were cotransfected in a suspension in 12-well tissue culture plates using Lipofectamine 2000. Each well contained 2 μg of the indicated pCAGGs VP16 and GAL4 expression plasmids, 1 μg of the reporter pG5 GFP/Luc plasmid, and 0.1 μg of the Renilla luciferase (RL) expression plasmid pRL SV40 (Promega) to normalize transfection efficiencies. Seventy-two hours posttransfection, fluorescence images were obtained to evaluate protein-protein interaction by GFP expression using a Zeiss fluorescence microscope. After the imaging, cell lysates were prepared to determine luciferase activities using the Promega dual-luciferase reporter assay and a Lumicount luminometer (Packard). Reporter gene activation (FFL) is expressed as fold induction over the negative control (pCAGGs VP16 and pCAGGs NP-GAL4) after normalization of transfection efficiencies with the RL expression plasmid pRL SV40. The percentage of interaction of LCMV NP mutants with the wild-type LCMV NP was calculated based on the wild-type NP-NP interaction (pCAGGs NP-VP16 and pCAGGs NP-GAL4). M2H experiments were performed in triplicate. The mean and standard deviation were calculated using Microsoft Excel software. Protein expression was analyzed by a Western blot as previously described.

BiFC assay. MDCK cells (10^5) were cotransfected in a suspension on coverslips with 1 μg of the indicated pCAGGs EYN and EYC plasmids using Lipofectamine 2000. Twenty-four hours posttransfection, cells were placed at 30°C and 5% CO_2 atmosphere for 3 h to allow maturation of reconstituted YFP (17). Cells were then fixed with 100% methanol for 5 min, permeabilized with 0.1% Triton X-100 for 10 min, and blocked in 2.5% bovine serum albumin (BSA) in 1× PBS for 1 h at room temperature. Samples were incubated for 1 h at 37°C with a 1:500 dilution in 2.5% BSA of a primary monoclonal antibody that recognizes only the reconstituted forms of GFP or YFP (AbCAM; AB1218). After incubation, cells were washed with 1× PBS and incubated with DAPI (4′,6-diamidino-2-phenylindole) (Research Organics) and a 1:1,000 dilution of a secondary goat anti-mouse IgG-Alexa Fluor 647 antibody (Invitrogen). The coverslips were mounted onto glass slides with Mowiol and analyzed using a 63× oil immersion objective and a Zeiss fluorescence microscope with Adobe Photoshop CS4 (v11.0) software. Representative images of at least three independent transfections are shown.

RESULTS

Assessing LCMV NP-NP interaction. The role of negative-stranded virus RNA NPs in nucleocapsid formation predicts the need for NP-NP interaction. This NP oligomerization probably plays a major role in the encapsidation of viral RNA, in the formation of RNP that, together with the L protein, participates in RNA replication and transcription (22, 39), and, by interaction with the matrix protein, in incorporation of these RNPs into matured infectious virions (23, 37, 43). To demonstrate the ability of the LCMV NP to interact with itself, we used three complementary approaches: coimmunoprecipitation (Co-IP), the mammalian two-hybrid (M2H) system, and the bimolecular fluorescence complementation (BiFC) assay. For Co-IP studies (Fig. 1), we generated either N- or C-terminally HA- and FLAG-tagged versions of the full-length, wild-type LCMV NP. We cotransfected 293T cells with different combinations of NP-expressing plasmids. At 48 h posttransfection, we prepared cell lysates for Co-IP assays (Fig. 1A). The different NPs were expressed to similar levels, as determined by a Western blot of total cell lysates using an anti-HA or anti-FLAG antibody (Fig. 1A, Input). Cell lysates were reacted with anti-FLAG or anti-HA affinity agarose gel, and immunoprecipitates were analyzed by a Western blot using anti-HA or anti-FLAG antibodies. NP-NP interaction was detected independently of the tagged versions of NPs used for Co-IP (Fig. 1A, lanes 2, 3, 7, and 8). We observed the presence of the heavy chain of IgG (marked by an asterisk) in FLAG immunoprecipitates probed with the anti-HA antibody because both antibodies were derived from the same species.

Next, we evaluated whether NP self-association required expression of the interacting molecules in proximity of each other within the same cellular environment. To that end, we transfected cells with NP-HA (lane 1) or NP-FLAG (lane 2) or with NP-HA and NP-FLAG together (lane 3). Forty-eight hours posttransfection, we prepared cell lysates for Co-IP assays. The different NPs were expressed to similar levels, as determined by a Western blot with an anti-HA or anti-FLAG antibody (Fig. 1B, Input). To evaluate NP-NP interaction *in vitro*, we mixed extracts from individually transfected cells (lane 4). Cell lysates were immunoprecipitated using an anti-FLAG antibody and analyzed by a Western blot using anti-HA or anti-FLAG antibodies. As expected, we did not observe the presence of NP in immunoprecipitates from individually transfected cells (Fig. 1B, lanes 1 and 2) but readily detected NP-HA in cells cotransfected with both tagged NP plasmids (Fig. 1B, lane 3). NPs produced in different cells did interact *in vitro* (Fig. 1B, lane 4).

To evaluate whether NP self-association was dependent on RNA (Fig. 1C), lysates from cells cotransfected with NP-HA and NP-FLAG were mock treated (Fig. 1C, lane 1), treated with RNase A/T1 (for single-stranded RNA) (Fig. 1C, lane 2), treated with RNase V1 (for double-stranded RNA) (Fig. 1C, lane 3), or treated with both RNase A/T1 and RNase V1 (Fig. 1C, lane 4). NP-NP interaction was not observed after treatment with RNase A/T1, whereas the interaction was not affected by treatment with RNase V1. This finding suggested that single-stranded RNA may play a role in NP self-association independently of the presence of genomic or antigenomic viral RNA.

We also determined the oligomeric state of the NP (Fig. 1D). To that end, cells were transfected with FLAG-NP, and 48 h later, cell lysates were prepared and analyzed by SDS-PAGE in the absence and in the presence of 2-mercaptoethanol (BME), followed by a Western blot using an antibody to FLAG. In the presence of BME, the LCMV NP migrated predominantly as a monomeric form with an approximate molecular mass of 55 kDa (Fig. 1D, +BME). In the absence of BME, the LCMV NP migrated predominantly as a higher-molecular-mass band of approximately 110 kDa (Fig. 1D, −BME), which likely corresponded to dimers of the NP. In the absence of BME, we also observed the presence of a lower-mobility band (molecular mass of approximately 180 kDa) that may represent a trimeric form of the LCMV NP, as well as a

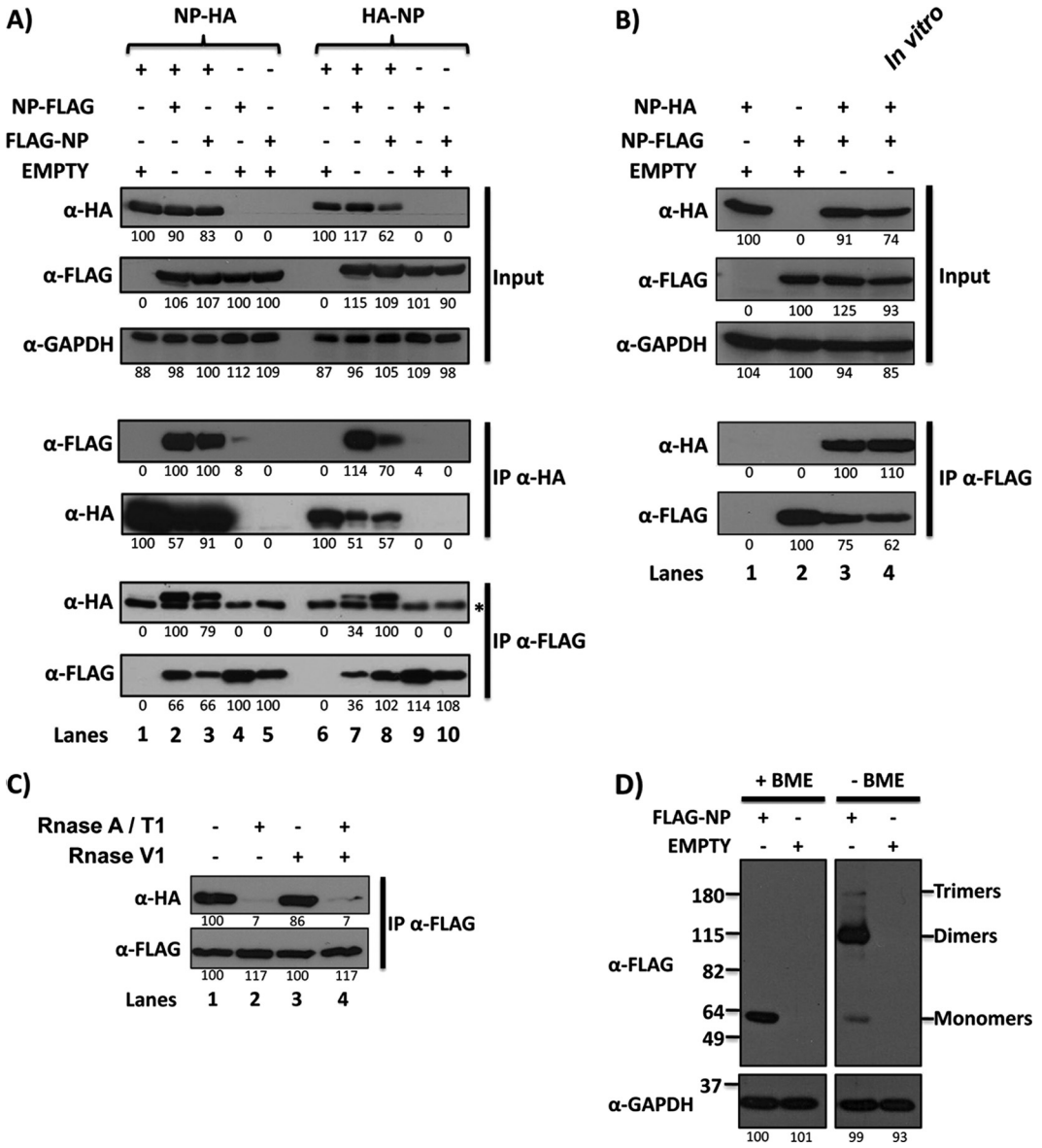

FIG 1 LCMV NP-NP interaction by coimmunoprecipitation (Co-IP). (A) 293T cells (3×10^6) were cotransfected in a 6-well tissue culture plate with 2.0 μg of the indicated expression plasmid encoding the full-length, wild-type LCMV NP tagged with HA at the N- and C-terminals (indicated as NP-HA and HA-NP, respectively) along with 2.0 μg of either the full-length, wild-type LCMV NP-FLAG (lanes 2 and 7) or the full-length, wild-type LCMV FLAG-NP (lanes 3 and 8). As negative controls for the interaction, HA- or FLAG-tagged versions of the LCMV NP were expressed individually (lanes 1, 4, 5, 6, 9 and 10). An empty pCAGGs MCS was used to normalize the amount of transfected DNA. Forty-eight hours posttransfection, cell lysates were prepared and analyzed for NP expression levels by a Western blot using anti-HA or anti-FLAG antibodies (Input). GAPDH was used as a loading control. Cell lysates were immunoprecipitated with anti-HA (IP α-HA) and anti-FLAG (IP α-FLAG) affinity agarose gels and analyzed by a Western blot as indicated on the left. An asterisk indicates the heavy chain of the anti-FLAG monoclonal antibody used for the IP. (B) *In vitro* reconstitution of NP-NP interaction. Extracts from individually plasmid-transfected cells were mixed and coimmunoprecipitated (lane 4, *in vitro*) with an anti-FLAG (IP α-FLAG) affinity agarose gel and analyzed by a Western blot with anti-HA and anti-FLAG polyclonal antibodies. Extracts from individually plasmid-transfected cells were included as negative controls (lane 1, NP-HA; lane 2, NP-FLAG). Extracts from cells cotransfected with both NP-HA and NP-FLAG were included as positive controls (lane 3). (C) RNase treatment. Extracts from cells cotransfected with 2 μg of pCAGGs NP-HA and NP-FLAG were mock treated (lane 1), treated with RNase A/T1 (lane 2), treated with RNase V1 (lane 3), or treated with all of the RNases (lane 4) prior to coimmunoprecipitation with the α-FLAG antibodies and a Western blot with α-HA and α-FLAG antibodies. (D) LCMV NP oligomerization. 293T cells were transfected with 2 μg of pCAGGs LCMV FLAG-NP. Forty-eight hours after transfection, cell extracts were prepared and analyzed by SDS-PAGE in the presence (+BME) and in the absence (−BME) of 2-mercaptoethanol. Empty pCAGGs MCS transfected cell extracts (empty) were included as a negative control. LCMV NP protein bands were analyzed by a Western blot using an α-FLAG polyclonal antibody. Protein molecular mass markers (kDa) are indicated on the left. The positions of NP monomers, dimers, and trimers are indicated on the right. GAPDH was used as a loading control. (A to D) Numbers at the bottom of each Western blot lane represent protein band intensities normalized to wild-type NP expression levels. Quantification of the bands was performed as described in Materials and Methods.

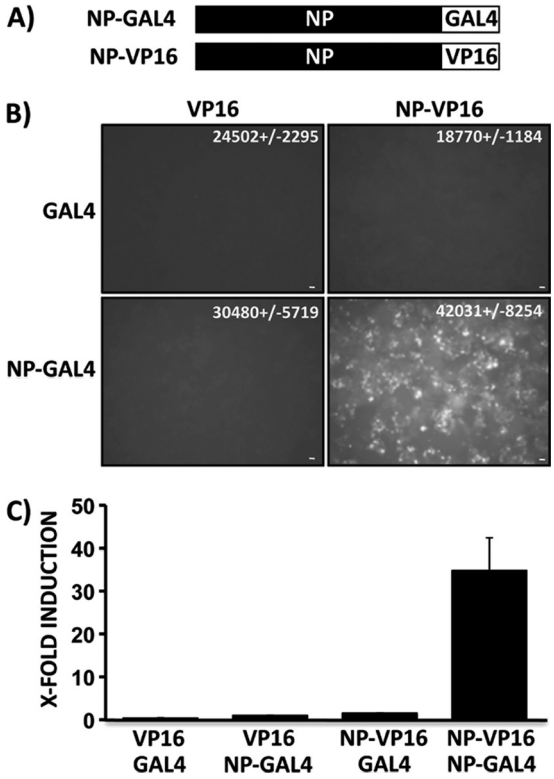

FIG 2 Assessing LCMV NP-NP interaction by the mammalian two-hybrid (M2H) system. (A) Schematic representation of the VP16- and GAL4-tagged versions of the LCMV NP that were used in the M2H system to detect NP-NP interaction. (B and C) NP-NP interaction. 293T cells (6.5×10^5) were cotransfected (12-well tissue culture plates) with 2 μg of the indicated expression plasmids, 1 μg of the dual reporter plasmid pG5 GFP/Luc, and 0.1 μg of the pRL SV40 expression vector to normalize transfection efficiencies. Seventy-two hours posttransfection, GFP expression was assessed using fluorescence microscopy (B) and cell extracts were prepared using the Promega dual-luciferase reporter assay and a Lumicount luminometer to determine the strength of the interaction (C). GAL4 and VP16 expression plasmids were used as negative controls. Reporter gene activation (FFL) is expressed as fold induction over the negative control (pCAGGs VP16 and pCAGGs NP-GAL4) after normalization of transfection efficiencies with the Renilla luciferase expression plasmid pRL SV40. Renilla luciferase values (means ± standard deviations) for each transfection are indicated in each image. Scale bar, 10 μm.

band of about 55 kDa corresponding to the monomeric form of the LCMV NP.

To confirm and quantify more accurately the property of the LCMV NP of self-association, we used the M2H approach (Fig. 2). To that end, we cotransfected 293T cells with pCAGGs plasmids expressing NP-GAL4 and NP-VP16 (Fig. 2A) together with the reporter plasmid pG5 GFP/Luc and pRL SV40 to normalize transfection efficiencies. NP-NP interaction would allow for GAL4 DNA binding to the reporter, while the VP16 activation domain recruits the machinery necessary for the expression of the GFP and FFL reporter genes. pCAGGs VP16 and GAL4 were used as negative controls alone or in combination with tagged NP expression plasmids to demonstrate the specificity of the NP-NP interaction. We detected NP self-association, as determined by both GFP (Fig. 2B) and FFL (Fig. 2C) reporter gene expression.

The arenavirus life cycle is restricted to the cell cytoplasm (7), and thereby, biologically meaningful NP-NP interactions are expected to take place in this subcellular compartment. To demonstrate that NP self-association occurs in the cell cytoplasm, we used the BiFC assay (Fig. 3). In this assay, the YFP amino acid sequence is split into two fragments: EYN, encoding the N-terminal domain (amino acids 1 to 155), and EYC, encoding the C-terminal domain (amino acids 156 to 239). EYN and EYC were then used to generate fusion constructs with the LCMV NP. An NP-NP interaction would result in restoration of the YFP ternary structure and its associated fluorescence, readily detected by fluorescence microscopy. We fused EYN and EYC to the N- and C-terminal ends of the LCMV NP (Fig. 3A) and confirmed their expression by a Western blot (Fig. 3B). In cells cotransfected with NP-EYN and NP-EYC, we observed YFP expression, which is indicative of NP-NP interaction (Fig. 3C, YFP) restricted to the cell cytoplasm. To confirm the YFP reconstitution, we used a monoclonal antibody against GFP or YFP that recognizes only the reconstituted ternary fluorescent protein structure (Fig. 3C, α-GFP MAb). Notably, the NP-NP interaction was not detected when either EYN or EYC was fused to the N terminus of the LCMV NP, a finding we also observed in the M2H assay when using N-terminally tagged versions of the NP (not shown). Taken together, these results demonstrated the ability of the LCMV NP to self-associate.

Assessing homotypic and heterotypic interactions among arenavirus NPs. We next investigated whether NP-NP interaction is a common feature among arenavirus NPs and also whether NPs from different arenavirus species are able to interact with each other (heterotypic interaction). For this, we chose to examine the interaction of the NP of the prototypic arenavirus LCMV with the NPs from two HF arenaviruses, the OW LASV and the NW MACV (Fig. 4). To test these interactions by Co-IP, we generated HA- and FLAG-tagged versions of the LASV NP (Fig. 4A) and the MACV NP (Fig. 4B) that were cotransfected alone or in combination with tagged versions of the LCMV NP into 293T cells. All tagged proteins were expressed at similar levels, as determined by a Western blot (Fig. 4A and 4B, Input α-HA and α-FLAG). Immunoprecipitation of cell lysates using anti-FLAG affinity agarose gels followed by Western blot analysis of immunoprecipitated proteins using an anti-HA antibody confirmed the homotypic interaction of the LASV NP (Fig. 4A, IP α-FLAG and α-HA, lane 7) and the MACV NP (Fig. 4B, IP α-FLAG and α-HA, lane 7). In addition, the LCMV NP interacted with the LASV NP (Fig. 4A, IP α-FLAG and α-HA, lanes 6 and 8) and with the MACV NP (Fig. 4B, IP α-FLAG and α-HA, lanes 6 and 8). Quantification of the immunoprecipitated protein bands suggested that the LCMV NP homotypic interaction was slightly stronger than its heterotypic interaction with the NP of MACV. These results suggested that a common domain(s) might be involved in homo- and heterotypic NP-NP interactions and that specific amino acid differences within this domain(s) may affect the strength of the NP-NP interaction.

To confirm these homo- and heterotypic NP-NP interactions, we used the M2H system (Fig. 5). To that end, we cotransfected 293T cells with the indicated combinations of LCMV, LASV, and MACV NP expression plasmids, fused to GAL4 and VP16, and the M2H reporter plasmid pG5 GFP/Luc and the pRL SV40 to normalize transfection efficiencies. The LASV NP interacted with itself and with the LCMV NP, as determined by GFP (Fig. 5A) and FFL (Fig. 5B) reporter gene expression. FFL expression levels did not show significant differences between LCMV and LASV NP homotypic interactions. We obtained similar results for NP-NP

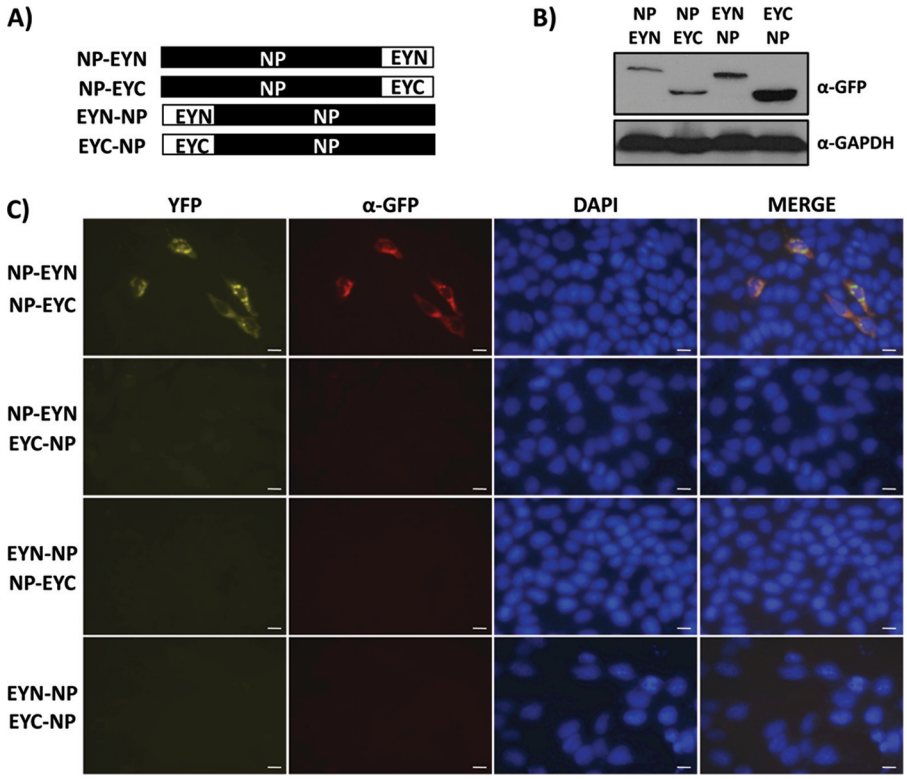

FIG 3 Detection of LCMV NP-NP interaction by the bimolecular fluorescence complementation (BiFC) assay. (A) Schematic representation of the EYN- and EYC-tagged versions of the LCMV NP used in the BiFC approach. (B) Protein expression levels. Tagged LCMV NPs were detected by a Western blot using an anti-GFP polyclonal antibody that detects the N- and C-terminal domains of YFPs present in plasmid constructs (α-GFP PAb). GAPDH was used as a loading control. (C) YFP reconstitution. MDCK cells (10^5) were cotransfected in 12-well tissue culture plates with the indicated plasmid combinations (left), incubated at 37°C for 24 h, and transferred to an incubator at 30°C for 3 h to allow maturation of YFP. YFP expression was detected by fluorescence microscopy (YFP) and by using an anti-GFP monoclonal antibody that recognizes only the reconstituted GFP or YFP (α-GFP MAb). DAPI was used for nuclear staining. Representative 63× images are shown. Scale bar, 10 μm.

interactions between LCMV and MACV (Fig. 5C and D). The results from our Co-IP and M2H assay suggested that NP self-association appears to be a common feature among arenavirus NPs. Likewise, our findings indicated that NP-NP heterotypic interactions can occur between genetically distantly related (OW and NW) arenaviruses, suggesting the possibility of a common interaction domain(s) that is conserved among different virus strains.

Identification of the NP domain that mediates NP-NP interaction. To identify the domain required for NP self-association, we used a series of previously described N-terminal (Fig. 6) and C-terminal (Fig. 7) LCMV NP deletion mutants (24) that were fused to VP16 and used, together with the wild-type LCMV NP fused to GAL4, in the M2H system. None of the LCMV NP N-terminal deletion (ΔN) mutants tested (Fig. 6A) interacted with the wild-type LCMV NP (Fig. 6B), suggesting that the N terminus is involved in NP-NP interaction. All the ΔN NP mutants tested, with the exception of ΔN200, which was expressed at significantly lower levels, were expressed at levels similar to those of the wild-type LCMV NP (Fig. 6C). Furthermore, the same N-terminal LCMV NP mutants have been proved to be functional in interactions with LCMV Z, suggesting, to some extent, their functionality (37). We next examined the ability of LCMV NP C-terminal deletion (ΔC) mutants to interact with the wild-type LCMV NP (Fig. 7A). Deletions of the last 200 amino acids did not compromise self-association of the LCMV NP; however, deletions of the last 250 amino acids disrupted the interaction (Fig. 7B). All C-terminal LCMV NP mutants, with the exception of ΔC250, were expressed at levels similar to those of the wild-type LCMV NP (Fig. 7C).

The anti-IFN function of the LCMV NP is not required for its self-assembly. We have previously shown that the C-terminal region of the LCMV NP is required for the anti-IFN activity of the NP (24). In particular, we documented that residues D382, G385, and R386 within the DIEGR motif were required for the anti-IFN function of the LCMV NP (24). Moreover, it has been recently shown that the LASV NP possesses a functional 3′ to 5′ exonuclease-folding domain within its C-terminal region, and residues located in the active site of the exonuclease domain were also required for counteracting the IFN response by the NP (16, 40). Since the NP-NP interaction and the anti-IFN domains mapped to different regions of the LCMV NP primary structure, we hypothesized that mutants incapable of counteracting the host cellular IFN response may still have normal NP-NP interaction. This hypothesis was supported by the rescue of a viable recombinant LCMV (though with significantly impaired fitness) carrying a D382A mutation in the NP that lacked the ability to counteract induction of the host type I IFN response (24). To further evaluate this hypothesis, we tested whether alanine substitutions in the residues involved in the active site of the LCMV NP exonuclease

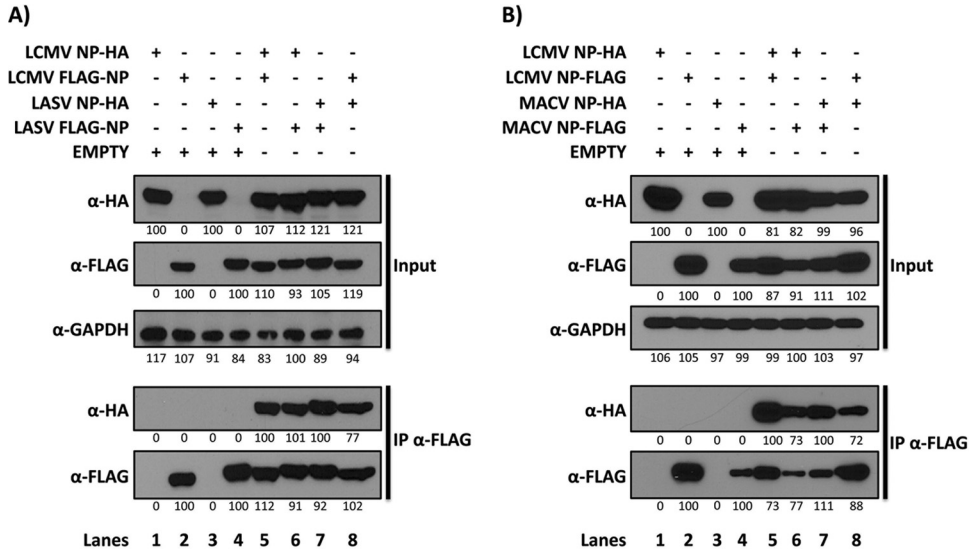

FIG 4 Arenavirus NP homotypic and heterotypic interactions. (A) Coimmunoprecipitation of the LCMV NP and the LASV NP. Equal amounts of plasmid DNA (2 μg) of LCMV and LASV NPs containing C-terminal HA or N-terminal FLAG tags were cotransfected individually (lanes 1 to 4) or in combinations (lanes 5 to 8) into 293T cells (3×10^6 per transfection) in 6-well tissue culture plates. An empty pCAGGs MCS plasmid was used to normalize the amount of total transfected DNA. After 48 h, cell lysates were prepared and analyzed for NP expression levels by a Western blot using anti-HA or anti-FLAG polyclonal antibodies (Input). GAPDH was used as a loading control. Cell lysates were coimmunoprecipitated using anti-FLAG affinity agarose gel (IP α-FLAG) and analyzed by a Western blot with either anti-HA or anti-FLAG polyclonal antibodies. (B) Coimmunoprecipitation of the LCMV NP and the MACV NP. Expression plasmids encoding LCMV and MACV NPs containing C-terminal HA and FLAG tags were cotransfected individually (lanes 1 to 4) or in combinations (lanes 5 to 8) as previously described. Input, NP expression levels; IP α-FLAG, coimmunoprecipitation analysis with anti-FLAG affinity gel. (A and B) Numbers at the bottom of each Western blot lane represent the quantification of band intensities normalized to wild-type NP expression levels as described in Materials and Methods.

domain (D382, E384, D459, H517, and D522A), as well as in G385A and R386A within the conserved DIEGR motif, with all of them known to be deficient in anti-IFN activity, retained their ability to interact with the wild-type LCMV NP by using the M2H approach (Fig. 8). As a control, we used the LCMV NP I383A mutant that we previously showed to retain its anti-IFN function (24). LCMV NP mutants deficient in anti-IFN were still able to interact with the wild-type LCMV NP at levels comparable to that of wild-type NP-NP interaction (Fig. 8A). All mutants were expressed to levels similar to that of the wild-type LCMV NP (Fig. 8B). These results indicated that the domain involved in NP self-association does not overlap with the anti-IFN function of the LCMV NP and that these two functions can be separated physically within the LCMV NP structure.

DISCUSSION

For many negative-strand RNA viruses, it has been shown that self-association of the virus nucleoprotein (NP) is required for the formation of the ribonucleoprotein core that directs both viral RNA replication and gene transcription (1, 13, 34, 42, 45). In this work, we have demonstrated that the NP of the prototypic arenavirus LCMV, as well as the NPs of OW LASV and NW MACV HF arenaviruses, has the property of self-association (homotypic interaction), a finding consistent with recent reports documenting the ability of the LASV (40) and NW arenavirus TCRV (23) NPs to form oligomeric structures. In addition, we have also documented heterotypic interactions among NPs from different arenavirus species.

The robustness of LCMV NP homotypic interaction was supported by obtaining similar findings using Co-IP (Fig. 1) and M2H (Fig. 2) assays. In addition, homotypic LCMV NP interaction was also confirmed by BiFC (Fig. 3) and shown to be restricted to the cell cytoplasm, as predicted based on the replication cycle of arenaviruses (7). In both the M2H (data not shown) and the BiFC assays, LCMV NP-NP interaction was detected only when the N-terminal domain of NP was untagged, suggesting a potential role of the N terminus in NP self-association. This NP self-association was also shown in NPs of OW LASV and NW MACV HF arenaviruses by Co-IP (Fig. 4) and M2H (Fig. 5) assays. In addition, we have also documented heterotypic interaction among NPs from different arenavirus species. Results from assays using a collection of LCMV NP N-terminal (Fig. 6) and C-terminal (Fig. 7) deletion mutants indicate the importance of the N-terminal domain of the LCMV NP for its self-association. Recently published findings for the TCRV NP showed that residues 19 to 119 in the N-terminal domain played a critical role in self-association of the TCRV NP protein. Our findings with the LCMV NP further confirm that residues 1 to 50 at the N terminus, as well as residues located within a region covering amino acids 308 to 358, are critical for LCMV NP self-association.

Our results have also shown that the NP self-association domain does not overlap with a previously identified domain responsible for the anti-IFN function of the LCMV NP (Fig. 8). Accordingly, these two functions can be separated physically in the LCMV NP structure. Thus, LCMV NP mutants lacking the anti-IFN activity interacted with the wild-type LCMV NP with strength similar to that of the wild-type NP-NP interaction. This is further supported by our previous finding that N-terminal deletion mutants affecting NP-NP interaction (e.g., deletions up to the 350 first amino acids) retained their ability to inhibit Sendai virus (SeV)-mediated induction of type I IFN (24). This, in turn, suggests that monomers of the NP could counteract the cellular host

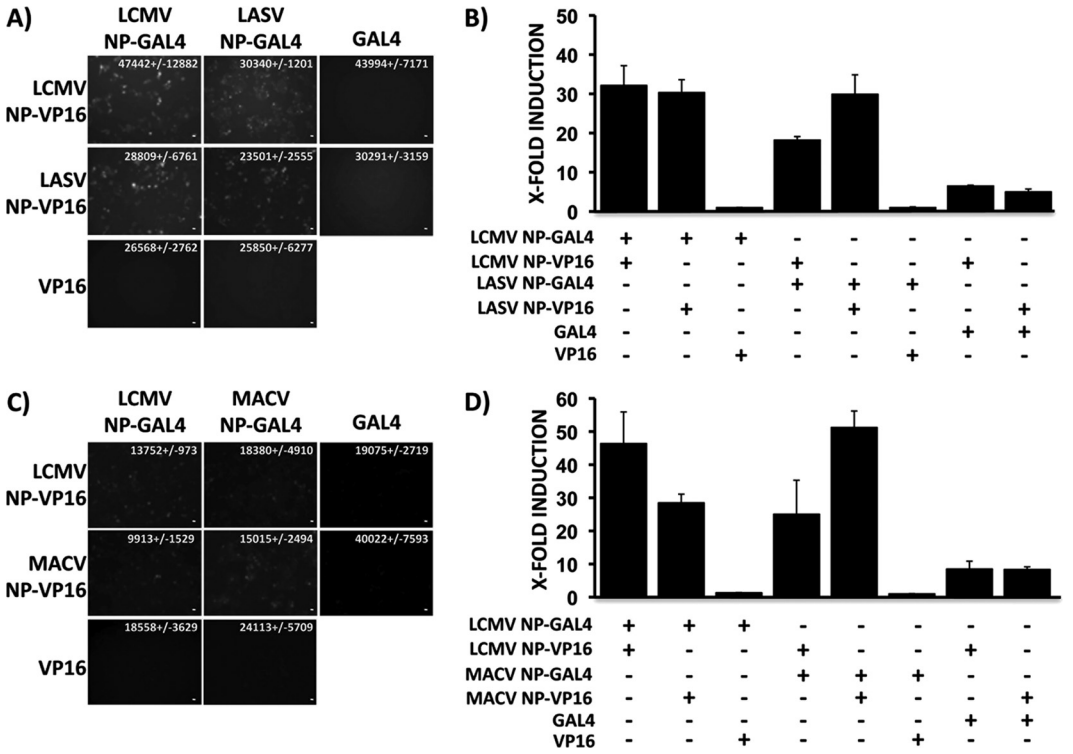

FIG 5 Assessing homotypic and heterotypic interactions among arenavirus NPs by the M2H system. 293T cells (6.5×10^5) were cotransfected, as previously described for Fig. 2, with plasmids fused to GAL4 and VP16 expressing the LCMV and LASV NPs (A and B) or the LCMV and MACV NPs (C and D). Seventy-two hours posttransfection, NP-NP interactions were detected by GFP expression using fluorescence microscopy for LCMV and LASV (A) or for LCMV and MACV (C). GAL4 and VP16 expression plasmids were used as negative controls. To quantify interactions, cell lysates were prepared and levels of luciferase expression were analyzed. Reporter gene activation (FFL) is expressed as fold induction over the negative transfected controls (pCAGGs VP16 and pCAGGs NP-GAL4) after normalization of transfection efficiencies with the pRL SV40 expression plasmid for LCMV and LASV (B) and LCMV and MACV (D) NP-NP interactions. Renilla luciferase values (means ± standard deviations) for each transfection are indicated in each image. Scale bar, 10 μm.

IFN response, raising the intriguing possibility that defined NP fragments often observed in virally infected cells may, despite not contributing to formation of functional RNPs, favor virus propagation by providing a decoy strategy against the host innate immune response (9, 15).

Our results and previous reports (23, 37) suggest the presence of two domains in arenavirus NPs in which the C-terminal domain is responsible for counteracting the host type I IFN response (24) and also for interaction with Z (23, 37, 43), with key residues involved in these two functions (37). On the other hand, the N-terminal domain would be involved in NP self-association (reference 23 and this study). However, a contribution of residues within the C-terminal region of the NP in NP-NP interaction cannot be ruled out. For instance, relevant residues within the C-terminal region of the NP may participate in stabilizing the N-terminal domain involved in the NP-NP interaction or the NP interaction with other viral or cellular proteins that create the appropriate structural conformation for the NP-NP interaction. This could explain some differences found in the magnitude of the interaction among C-terminal deletion mutants as well as differences observed in heterotypic NP-NP interactions. We (and others) have recently demonstrated a similar situation with the influenza IFN antagonist nonstructural protein 1 (NS1) (10, 21). A second domain (amino acids 103 and 106) in the middle of NS1 was identified for binding to the cleavage and polyadenylation specificity factor (CPSF) in combination with the conventional CPSF interaction site located at the C terminus of NS1 (32, 36, 46).

Based on the recently described crystal structure of the LASV NP, Qi et al. suggested that NP self-association occurs through N- to C-terminal interactions (40). At first glance, our results (and those found with the TCRV NP [23]) are difficult to reconcile with this model. It is plausible that self-association of arenavirus NPs may require interaction between other interfaces in addition to those suggested by the crystal structure and for which the N-terminal region may play a major role. One potential scenario that would help to reconcile both models is that NP self-association is mediated by two different mechanisms. One involves head-to-tail interactions (as suggested by the crystal structure model) and the other involves an RNA-based bridge through the N-terminal domain of the NP (as suggested by the biochemical results). This model would explain why N-terminal mutants are not able to self-associate or interact with RNA. On the other hand, in this model, C-terminal mutants would lose the NP-NP interaction domain at the C-terminal end but still be able to interact with RNA and, therefore, still be able to show NP self-association. Recently, the LASV NP quaternary structure has been determined (6). These studies uncovered asymmetric and symmetric trimeric structures of the LASV NP with a tail-to-tail (N-N) interface and a head-to-tail (C-N) interface, respectively. Electron microscopy and small-angle X-ray scattering analysis favor the NP association into a symmetric complex in solution, suggesting that C-N interactions reflect true interactions between NP monomers in solution without excluding the possibility that upon binding to RNA or after posttranslational modifications, the NP could reorganize,

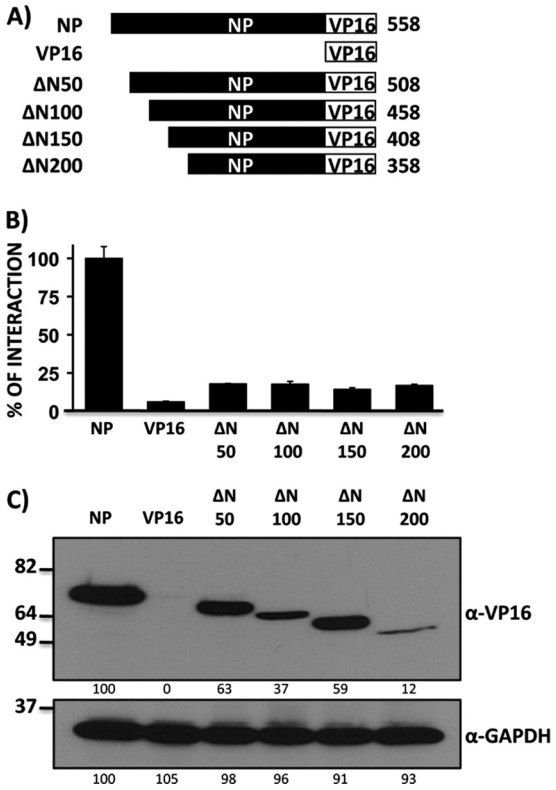

FIG 6 The N-terminal region of the LCMV NP is involved in NP-NP interaction. (A) Schematic representation of the LCMV NP N-terminal deletion mutants used in the M2H system. Total amino acid lengths of the NP wild-type and deletion mutants are indicated on the right. (B) LCMV NP-NP interaction with N-terminal deletion mutants. 293T cells (6.5×10^5) were cotransfected as previously described in Fig. 2, and 72 h posttransfection, NP-NP interactions were quantified in cell lysates. Reporter gene activation (FFL) was determined by fold induction over the negative transfected control (pCAGGs VP16 and pCAGGs NP-GAL4) after normalization of transfection efficiencies with the pRL SV40 expression plasmid. The percentage of interaction between each of the LCMV NP mutants with wild-type LCMV NP was calculated based on wild-type NP-NP interaction (pCAGGs NP-VP16 and pCAGGs NP-GAL4). (C) Protein expression levels of LCMV NP mutants. Cell lysates were used to detect expression of LCMV NP wild-type and N-terminal deletion mutants by a Western blot using an anti-VP16 polyclonal antibody. GAPDH was used as a loading control. Protein molecular mass markers (kDa) are indicated on the left. Numbers at the bottom of each Western blot lane represent the quantification of band intensities normalized to wild-type NP expression levels as described in Materials and Methods.

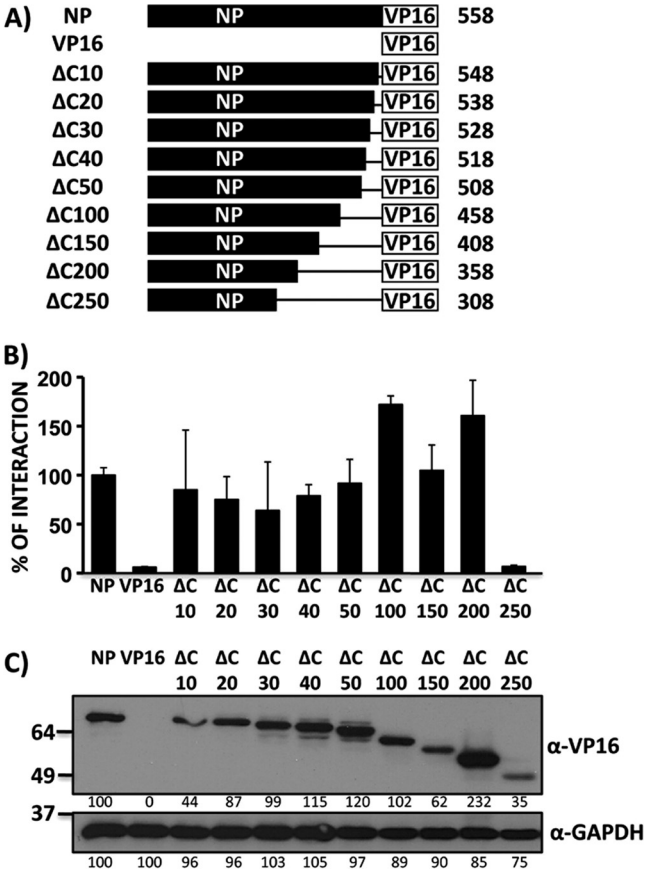

FIG 7 The last 200 amino acids in the C-terminal region of the LCMV NP are not required for NP-NP interaction. (A) Schematic representation of LCMV NP wild-type and C-terminal deletion mutants used in the M2H system. Total amino acid lengths of NP wild-type and deletion mutants are indicated on the right. (B) LCMV NP-NP interaction with C-terminal deletion mutants. 293T cells (6.5×10^5) were cotransfected, and the presence of NP-NP interaction was quantified in cell lysates as described for Fig. 6. The percentage of interaction between each of the C-terminal deletion mutants with wild-type LCMV NP was calculated based on wild-type NP-NP interaction (pCAGGs NP-VP16 and pCAGGs NP-GAL4).(C) Expression levels of LCMV NP mutants. The same cell lysates were used to detect expression of LCMV NP wild-type and C-terminal deletion mutants by a Western blot using a polyclonal anti-VP16 antibody. GAPDH was used as a loading control. Protein molecular mass markers (kDa) are indicated on the left. Numbers at the bottom of each Western blot lane represent the quantification of band intensities normalized to wild-type NP expression levels as described in Materials and Methods.

forming other structures (6). Future studies are required to demonstrate this hypothesis and to explain these apparent discrepancies between biochemical results and predictions derived from the crystal structure of the LASV NP. Although in our assays we did not include a specific LCMV RNA sequence that can facilitate NP self-association, we cannot exclude the possibility that LCMV NP mRNA produced by the pCAGGs expression plasmid is specifically recognized by the LCMV NP. It should be noted that this nucleus-generated, plasmid-derived LCMV NP mRNA contains features, including a distinct 3′ untranslated region (UTR) and poly(A) tail, that are missing in the viral mRNAs produced in the cytoplasm of LCMV-infected cells. Alternatively, the interaction of the NP with RNA may not require viral RNA and could be mediated by an unspecific cellular RNA. Whether NP self-association is required for binding RNA and whether monomers of NP bind to RNA remain to be determined. Intriguingly, previous studies with the TCRV NP suggested that NP-NP interaction was RNA independent, a result which appears counterintuitive for a negative-strand RNA virus.

We have previously shown that N-terminal deletions in the NP abrogated its ability to promote RNA replication and gene expression of an LCMV minigenome (MG) (24). This finding may, at least partly, reflect an inability of these NP mutants to generate functional nucleocapsids due to their lacking the self-association property. It needs to be further evaluated whether NP self-association is required for RNA binding and transcriptional activities of RNP complexes. Our results also showed that deletions in the C-terminal region of the NP did not affect NP self-association, but C-terminal deletions were shown to abrogate NP functions

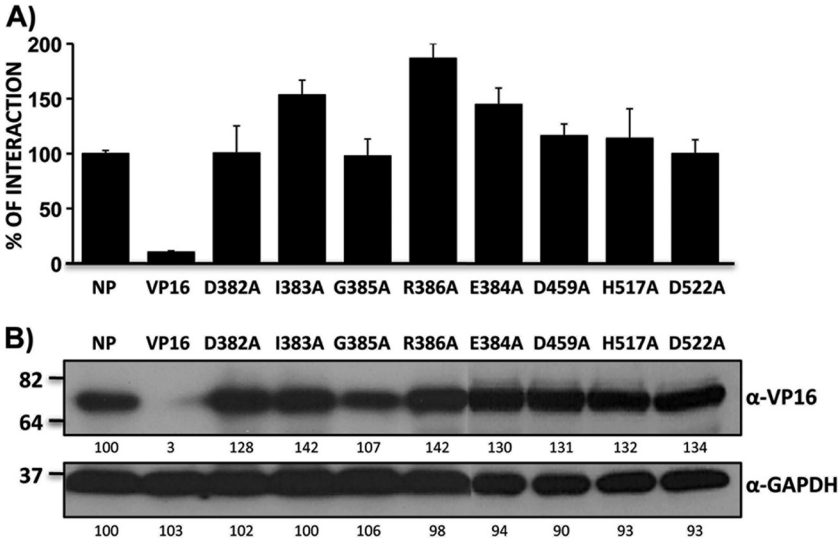

FIG 8 Critical amino acid residues required for the anti-IFN function of the LCMV NP are not required for NP-NP interaction. (A) 293T cells (6.5×10^5) were cotransfected as indicated in Fig. 2, and interactions of the DIEGR motif and the catalytic site of the 3′ to 5′ exonuclease motif mutants with wild-type LCMV NPs were quantified in cell lysates as described in Fig. 6. The percentage of interaction between each of the single-amino-acid mutants with wild-type LCMV NP was calculated based on wild-type NP-NP interaction (pCAGGs NP-VP16 and pCAGGs NP-GAL4). (B) Expression levels of LCMV NP mutants. The same cell lysates were used to detect expression of LCMV wild-type NP and single-amino-acid mutants by a Western blot using a polyclonal anti-VP16 antibody. GAPDH was used as a loading control. Protein molecular mass markers (kDa) are indicated on the left. Numbers at the bottom of each Western blot lane represent the quantification of band intensities normalized to wild-type NP expression levels as described in Materials and Methods.

required for replication and transcription of an LCMV minigenome (24). These results suggest that the C-terminal region of the NP might have a direct role in transcription and replication that is independent of nucleocapsid formation. As previously reported (24), the overall structural integrity of the LCMV NP is probably required for its involvement in replication and transcription.

NPs are highly conserved among members in the *Arenaviridae* family, and comparisons between the LCMV NP and the LASV NP and between the LCMV NP and the MACV NP show 61% and 50% amino acid sequence identities, respectively, that increase to 66% and 56% when comparing only the 350-amino-acid N-terminal region (ClustalW2 analysis). Our studies have also shown that the LCMV NP interacts with the LASV NP and with the MACV NP, but homotypic interactions were slightly stronger than heterotypic NP-NP interactions, indicating that specific amino acid residues may be required for a proper NP-NP interaction. Our findings, however, suggest a possible protein domain that is common among even distantly related arenaviruses and which may potentially provide a target for antiviral development against all members in the family. The identification of specific amino acid residues within the NP that are directly involved in NP-NP interaction may facilitate the design of peptides able to disrupt NP-NP interaction and affect virus RNA synthesis, as previously documented for other viruses (47). Likewise, it would be feasible to develop assays amenable to high-throughput screening (HTS) technologies to identify small molecule inhibitors affecting NP-NP interaction that may be active against most, or all, human pathogenic arenaviruses.

ACKNOWLEDGMENTS

We thank members of L.M.-S.'s laboratory for their discussions and Snezhana Dimitrova for technical support. We acknowledge Adolfo García-Sastre and Juan Ayllón (Mount Sinai School of Medicine, NY) for the BiFC plasmids and technical advice. We also thank Alba Guarne (Health Sciences Centre, McMaster University) for valuable discussions.

E.O.-R. is a Fulbright-Conicyt fellowship recipient (BIO 2008). Research in L.M.-S.'s laboratory was partially funded by NIAID grant RO1AI077719. Research at J.C.D.L.T.'s laboratory was supported by grants RO1AI047140, RO1AIO77719, and RO1AI079665 from the NIH/NIAID.

REFERENCES

1. **Albertini AA, et al.** 2006. Crystal structure of the rabies virus nucleoprotein-RNA complex. Science **313**:360–363.
2. **Barton LL.** 1996. Lymphocytic choriomeningitis virus: a neglected central nervous system pathogen. Clin. Infect. Dis. **22**:197.
3. **Borio L, et al.** 2002. Hemorrhagic fever viruses as biological weapons: medical and public health management. JAMA **287**:2391–2405.
4. **Borrow P, Martinez-Sobrido L, de la Torre JC.** 2010. Inhibition of the type I interferon antiviral response during arenavirus infection. Viruses **2**:2443–2480.
5. **Borrow P, Oldstone MB.** 1994. Mechanism of lymphocytic choriomeningitis virus entry into cells. Virology **198**:1–9.
6. **Brunotte L, et al.** 2011. Structure of the Lassa virus nucleoprotein revealed by X-ray crystallography, small-angle X-ray scattering, and electron microscopy. J. Biol. Chem. **286**:38748–38756.
7. **Buchmeier MJ, de la Torre JC, Peters CJ.** 2007. Arenaviridae: the viruses and their replication, p 1791–1827. *In* Knipe DM, et al (ed), Fields virology, 5th ed, vol 2. Lippincott Williams & Wilkins, Philadelphia, PA.
8. **Charrel RN, de Lamballerie X.** 2003. Arenaviruses other than Lassa virus. Antiviral Res. **57**:89–100.
9. **Clegg JC, Lloyd G.** 1983. Structural and cell-associated proteins of Lassa virus. J. Gen. Virol. **64**:1127–1136.
10. **Das K, et al.** 2008. Structural basis for suppression of a host antiviral response by influenza A virus. Proc. Natl. Acad. Sci. U. S. A. **105**:13093–13098.
11. **Eichler R, et al.** 2004. Characterization of the Lassa virus matrix protein Z: electron microscopic study of virus-like particles and interaction with the nucleoprotein (NP). Virus Res. **100**:249–255.
12. **Fischer SA, et al.** 2006. Transmission of lymphocytic choriomeningitis virus by organ transplantation. N. Engl. J. Med. **354**:2235–2249.

13. **Green TJ, Zhang X, Wertz GW, Luo M.** 2006. Structure of the vesicular stomatitis virus nucleoprotein-RNA complex. Science **313**:357–360.
14. **Gunther S, Lenz O.** 2004. Lassa virus. Crit. Rev. Clin. Lab. Sci. **41**:339–390.
15. **Harnish DG, Leung WC, Rawls WE.** 1981. Characterization of polypeptides immunoprecipitable from Pichinde virus-infected BHK-21 cells. J. Virol. **38**:840–848.
16. **Hastie KM, Kimberlin CR, Zandonatti MA, MacRae IJ, Saphire EO.** 2011. Structure of the Lassa virus nucleoprotein reveals a dsRNA-specific 3′ to 5′ exonuclease activity essential for immune suppression. Proc. Natl. Acad. Sci. U. S. A. **108**:2396–2401.
17. **Hu CD, Kerppola TK.** 2003. Simultaneous visualization of multiple protein interactions in living cells using multicolor fluorescence complementation analysis. Nat. Biotechnol. **21**:539–545.
18. **Isaacson M.** 2001. Viral hemorrhagic fever hazards for travelers in Africa. Clin. Infect. Dis. **33**:1707–1712.
19. **Jahrling PB, Peters CJ.** 1992. Lymphocytic choriomeningitis virus. A neglected pathogen of man. Arch. Pathol. Lab. Med. **116**:486–488.
20. **Kilgore PE, et al.** 1997. Treatment of Bolivian hemorrhagic fever with intravenous ribavirin. Clin. Infect. Dis. **24**:718–722.
21. **Kochs G, Garcia-Sastre A, Martinez-Sobrido L.** 2007. Multiple anti-interferon actions of the influenza A virus NS1 protein. J. Virol. **81**:7011–7021.
22. **Lee KJ, Novella IS, Teng MN, Oldstone MB, de La Torre JC.** 2000. NP and L proteins of lymphocytic choriomeningitis virus (LCMV) are sufficient for efficient transcription and replication of LCMV genomic RNA analogs. J. Virol. **74**:3470–3477.
23. **Levingston Macleod JM, et al.** 2011. Identification of two functional domains within the arenavirus nucleoprotein. J. Virol. **85**:2012–2023.
24. **Martinez-Sobrido L, et al.** 2009. Identification of amino acid residues critical for the anti-interferon activity of the nucleoprotein of the prototypic arenavirus lymphocytic choriomeningitis virus. J. Virol. **83**:11330–11340.
25. **Martinez-Sobrido L, Giannakas P, Cubitt B, Garcia-Sastre A, de la Torre JC.** 2007. Differential inhibition of type I interferon induction by arenavirus nucleoproteins. J. Virol. **81**:12696–12703.
26. **Martinez-Sobrido L, Zuniga EI, Rosario D, Garcia-Sastre A, de la Torre JC.** 2006. Inhibition of the type I interferon response by the nucleoprotein of the prototypic arenavirus lymphocytic choriomeningitis virus. J. Virol. **80**:9192–9199.
27. **McCormick JB, Fisher-Hoch SP.** 2002. Lassa fever. Curr. Top. Microbiol. Immunol. **262**:75–109.
28. **McCormick JB, et al.** 1986. Lassa fever. Effective therapy with ribavirin. N. Engl. J. Med. **314**:20–26.
29. **McKee KT, Jr, Huggins JW, Trahan CJ, Mahlandt BG.** 1988. Ribavirin prophylaxis and therapy for experimental argentine hemorrhagic fever. Antimicrob. Agents Chemother. **32**:1304–1309.
30. **Mets MB, Barton LL, Khan AS, Ksiazek TG.** 2000. Lymphocytic choriomeningitis virus: an underdiagnosed cause of congenital chorioretinitis. Am. J. Ophthalmol. **130**:209–215.
31. **Munoz-Jordan JL, et al.** 2005. Inhibition of alpha/beta interferon signaling by the NS4B protein of flaviviruses. J. Virol. **79**:8004–8013.
32. **Nemeroff ME, Barabino SM, Li Y, Keller W, Krug RM.** 1998. Influenza virus NS1 protein interacts with the cellular 30 kDa subunit of CPSF and inhibits 3′ end formation of cellular pre-mRNAs. Mol. Cell **1**:991–1000.
33. **Neuman BW, et al.** 2005. Complementarity in the supramolecular design of arenaviruses and retroviruses revealed by electron cryomicroscopy and image analysis. J. Virol. **79**:3822–3830.
34. **Ng AK, et al.** 2008. Structure of the influenza virus A H5N1 nucleoprotein: implications for RNA binding, oligomerization, and vaccine design. FASEB J. **22**:3638–3647.
35. **Niwa H, Yamamura K, Miyazaki J.** 1991. Efficient selection for high-expression transfectants with a novel eukaryotic vector. Gene **108**:193–199.
36. **Noah DL, Twu KY, Krug RM.** 2003. Cellular antiviral responses against influenza A virus are countered at the posttranscriptional level by the viral NS1A protein via its binding to a cellular protein required for the 3′ end processing of cellular pre-mRNAs. Virology **307**:386–395.
37. **Ortiz-Riano E, Cheng BYH, de la Torre JC, Martinez-Sobrido L.** 2011. The C-terminal region of lymphocytic choriomeningitis virus nucleoprotein contains distinct and segregable functional domains involved in NP-Z interaction and counteraction of the type I interferon response. J. Virol. **85**:13038–13048.
38. **Peters CJ.** 2002. Human infection with arenaviruses in the Americas. Curr. Top. Microbiol. Immunol. **262**:65–74.
39. **Pinschewer DD, Perez M, de la Torre JC.** 2003. Role of the virus nucleoprotein in the regulation of lymphocytic choriomeningitis virus transcription and RNA replication. J. Virol. **77**:3882–3887.
40. **Qi X, et al.** 2010. Cap binding and immune evasion revealed by Lassa nucleoprotein structure. Nature **468**:779–783.
41. **Rodriguez M, McCormick JB, Weissenbacher MC.** 1986. Antiviral effect of ribavirin on Junin virus replication in vitro. Rev. Argent. Microbiol. **18**:69–74.
42. **Rudolph MG, et al.** 2003. Crystal structure of the Borna disease virus nucleoprotein. Structure **11**:1219–1226.
43. **Shtanko O, et al.** 2010. A role for the C terminus of Mopeia virus nucleoprotein in its incorporation into Z protein-induced virus-like particles. J. Virol. **84**:5415–5422.
44. **Snell N.** 1988. Ribavirin therapy for Lassa fever. Practitioner **232**:432.
45. **Tawar RG, et al.** 2009. Crystal structure of a nucleocapsid-like nucleoprotein-RNA complex of respiratory syncytial virus. Science **326**:1279–1283.
46. **Twu KY, Noah DL, Rao P, Kuo RL, Krug RM.** 2006. The CPSF30 binding site on the NS1A protein of influenza A virus is a potential antiviral target. J. Virol. **80**:3957–3965.
47. **Wu WW, Sun YH, Pante N.** 2007. Nuclear import of influenza A viral ribonucleoprotein complexes is mediated by two nuclear localization sequences on viral nucleoprotein. Virol. J. **4**:49.